Title

M cell-derived vesicles suggest a unique pathway for trans-epithelial antigen delivery

Journal

Tissue Barriers, 3(1-2)

ISSN

2168-8362

Authors

Sakhon, Olivia S
Ross, Brittany
Gusti, Veronica
et al.

Publication Date

2015-04-03

DOI

10.1080/21688370.2015.1004975

Peer reviewed

RESEARCH PAPER

Tissue Barriers 3:1-2, e1004975; January-June 2015; © 2015 Taylor & Francis Group, LLC

M cell-derived vesicles suggest a unique pathway for trans-epithelial antigen delivery

Olivia S Sakhon†, Brittany Ross†, Veronica Gusti, An Joseph Pham, Kathy Vu, and David D Lo*

Division of Biomedical Sciences; School of Medicine; University of California, Riverside; Riverside, CA USA

†These authors contributed equally to this work.

Keywords: cytoplasm, M cell, PGRP-S-dsRed/CX_3CR1-EGFP double transgenic mice, Peyer's patch, immune surveillance, vesicle

Abbreviations: MCM, M cell-derived microvesicle; TLR2, toll-like receptor 2; TLR4, toll-like receptor 4

M cells are a subset of mucosal epithelial cells with specialized capability to transport antigens across the mucosal barrier, but there is limited information on antigen transfer in the subepithelial zone due to the challenges in tracking microparticles and antigens that are transcytosed by this unique cell. Using transgenic reporter mice expressing dsRed in the cytoplasm of M cells and EGFP in myeloid cells, we observed that the M cell basolateral pocket hosts a close interaction between B lymphocytes and dendritic cells. Interestingly, we identified a population of previously undescribed M cell-derived vesicles (MCM) that are constitutively shed into the subepithelial space and readily taken up by $CX_3CR1^+CD11b^+$ $CD11c^+$ dendritic cells. These MCM are characterized by their cytoplasmic dsRed confirming their origin from the M cell cytoplasm. MCM showed preferential colocalization in dendritic cells with transcytosed bacteria but not transcytosed polystyrene beads, indicating a selective sorting of cargo fate in the subepithelial zone. The size and number of MCM were found to be upregulated by bacterial transcytosis and soluble toll-like receptor 2 (TLR2) agonist, further pointing to dynamic regulation of this mechanism. These results suggest that MCM provide a unique function by delivering to dendritic cells, various materials such as M cell-derived proteins, effector proteins, toxins, and particles found in the M cell cytoplasm during infection or surveillance.

Introduction

Immune surveillance of mucosal sites, such as the intestine, is mainly focused at organized lymphoid tissues including the Peyer's patches and Isolated Lymphoid Follicles.[1-3] However, it can also occur by the direct sampling of the small intestine lumen by dendritic cells and goblet cells.[4,5] Among the epithelial cells overlying these tissues is a specialized subset of epithelial cells called M cells. They are morphologically distinct for their lack of apical brush border microvilli and the presence of a basolateral pocket occupied by B lymphocytes.[1,6] M cells are particularly efficient at capturing luminal microparticles and transporting them across the epithelial barrier ("transcytosis") for delivery to underlying antigen presenting cells.[1]

The mechanisms of microparticle capture and transcytosis may involve a number of distinct pathways. Transcytosis begins at the luminal face, where the M cell first encounters or captures particles.[7] This uptake can involve phagocytosis, macropinocytosis, or receptor mediated intake, although the relative contribution of each mechanism is not known.[8,9] Studies have identified receptor-mediated uptake mechanisms and non-receptor mediated uptake, as in the case of synthetic particles.[10-16] In extreme cases, it has even been suggested that some pathogens directly destroy the M cells, leaving gaps in the epithelial barrier.[17] Once inside the M cell, the cargo is rapidly transported across the cell. The machinery used for large particle apical-to-basolateral transport has not been clearly identified, since analogous mechanisms are not known for other epithelial cells. Moreover, it is not clear that the same mechanisms are used for all types of cargo.[18–20]

Once the particle reaches the basolateral side, it is thought to be released by the M cell for uptake by antigen sampling dendritic cells and lymphocytes (e.g., naïve B lymphocytes).[21–23] Transcytosis and delivery to antigen presenting cells have been difficult to address as there are significant challenges to studying these processes. Currently, studies on live or explanted Peyer's patch epithelium have not been able to examine transcytosis mechanisms with sufficient resolution to identify cellular pathways or mechanisms of delivery to dendritic cell. Other studies have used cell culture models to mimic M cell function, but it is not clear to what extent these models reflect *in vivo* mechanisms, and they cannot replicate the interactions with underlying dendritic cells.[24-26]

Due to the notable role of M cells as immunological portals, a variety of components may be found in the M cell cytoplasm

*Correspondence to: David D Lo; Email: david.lo@ucr.edu
Submitted: 11/09/2014; Revised: 12/23/2014; Accepted: 12/26/2014
http://dx.doi.org/10.1080/21688370.2015.1004975

intended for delivery to cells on the basolateral side. Release of both M cell cytoplasmic contents and disseminated foreign particles may involve the delivery of cargo packaged within vesicles. In recent years, the study of vesicles and their role during exposure to microorganisms has escalated quickly. Among phagocytic cells, 50—100 nm diameter vesicles were shown to be released from *Mycobacterium, Toxoplasma*, and *Salmonella* infected macrophages.[27] These vesicles contained microorganismal antigens and inflammatory cytokines. Additionally, vesicles may also include viral proteins, as was seen with HIV.[28] Released vesicles that may carry proteins, from either the host or microorganisms, can shape the response to the microbes.[29] Timar et al. identified antibacterial properties associated with vesicle production during the exposure of granulocytes to bacteria.[30]

In this report, we characterize a previously undescribed vesicle produced by M cells in the Peyer's patch follicle-associated epithelium, called M cell-derived microvesicles (MCM). As a first step toward *in vivo* analysis of MCM, we employed a PGRP-S-dsRed transgenic mouse model in which M cells specifically express a red reporter fluorescent protein (dsRed) in the cytoplasm. Reporter fluorescent proteins provide a useful way to mark the cytoplasm of each cell type, thereby delineating the boundaries of the cells and tracking the delivery of MCM to the subepithelial space. Using fluorescent bacteria, synthetic particles, and soluble agonists we were able to follow MCM movement from M cells to dendritic cells and compare this to transcytosed microparticles. Our studies suggest that MCM are distinct M cell structures that can be involved in immune surveillance.

Results

Double transgenic reporter mice allow for the visualization of M cells with dendritic cells and lymphocytes *in vivo*

We recently developed a transgenic reporter mouse strain, PGRP-S-dsRed, which expresses the red fluorescent protein dsRed under the control of the Peptidoglycan Recognition Protein-S (PGRP-S), resulting in expression specifically targeted to M cells of mucosal organized lymphoid tissues, as well as in circulating neutrophils.[31] We crossed the PGRP-S-dsRed mouse strain with CX_3CR1 (fractalkine receptor)- EGFP knock-in mice which express EGFP in myeloid cells, generating double transgenic mice with cytoplasmic expression of dsRed in M cells and EGFP in dendritic cells within mucosal lymphoid tissues. In these mice, M cells in intestinal Peyer's patch epithelium are columnar in shape with a basal invagination identified as the basolateral pocket (**Fig. 1A**). Further, staining with the B220/CD45R antibody highlighted the presence of B cells, both in the M cell basolateral pocket and in the follicle. Using 3-dimensional projections of confocal microscopy data, the intimate interaction between $EGFP^+$ dendritic cells within the basolateral pocket of M cells was clearly observed. Processes from dendritic cells can be seen extending into the subepithelial space, as well as from inside the pocket itself.

A similar relationship was also observed in Nasal Associated Lymphoid Tissue (NALT)

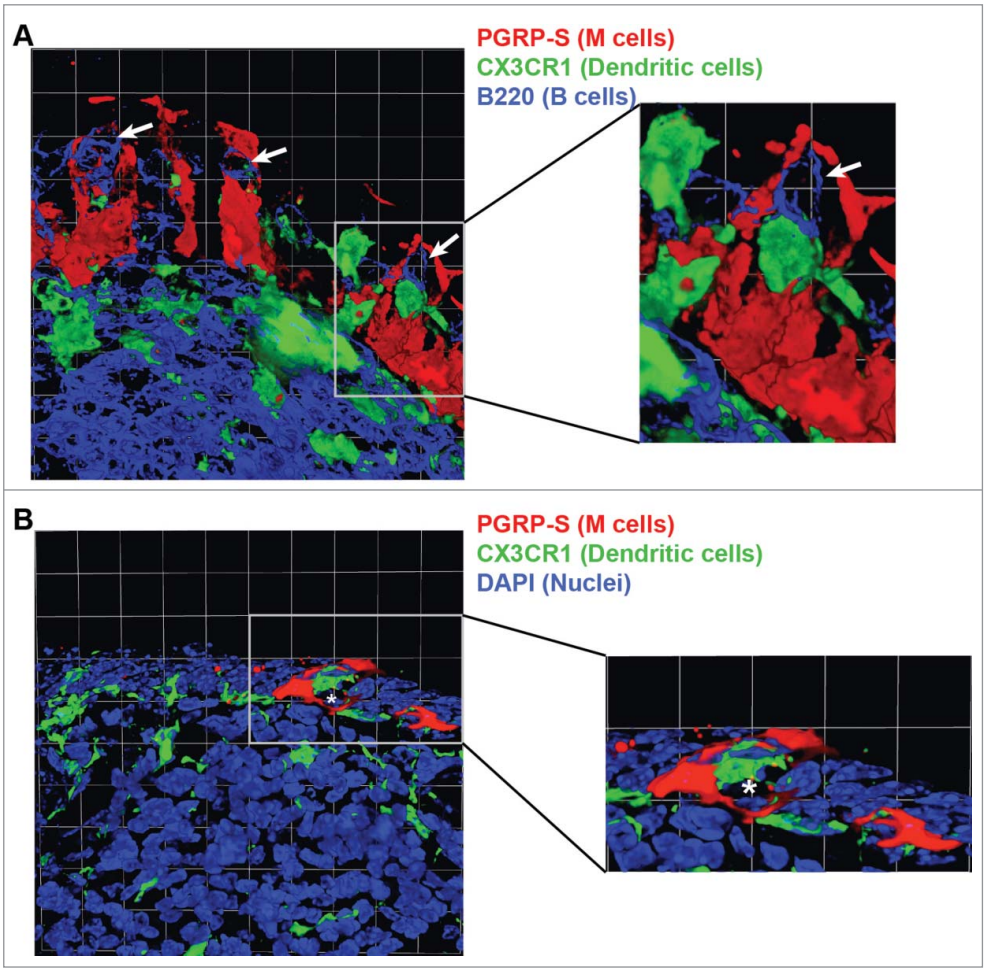

Figure 1. Transgenic reporters allow for *in vivo* visualization of the basolateral pocket. (**A**) Peyer's patch and (**B**) Nasal associated lymphoid tissue (NALT) were extracted from PGRP-S-dsRed/CX_3CR1-EGFP double transgenic mice. In the Peyer's patch (**A**), M cells express dsRed (red), dendritic cells express EGFP (green), and B cells (arrows) were stained with anti-B220/CD45R (blue). In the NALT (**B**), M cells express dsRed (red), myeloid cells express EGFP (green), and nuclei were stained with DAPI (blue). Basolateral pocket (asterisk). Scale: 1 grid unit = 13 μm. Experiments were performed at least 3 times with an *n* of at least 3 for each group.

(**Fig. 1B**), although in contrast to intestinal Peyer's patches, M cells here were flatter, reflecting their closer relationship to ciliated airway epithelium.[31] Despite this difference however, NALT M cells still exhibited basolateral pockets with closely integrated dendritic cells. Thus, regardless of developmental origin, M cells associated with organized lymphoid tissues showed intimate anatomic associations with underlying dendritic cells.

M cell expression of dsRed marks vesicles in the subepithelial space

We noted that a consistent feature of the subepithelial region in these mice was the appearance of small red fluorescent vesicles below the M cells, but not in the neighboring lamina propria outside the lymphoid tissue (**Fig. 2**). These vesicles were predominantly found within $CD11c^+$ subepithelial dendritic cells (**Fig. 2A**). They were also found within the $CX_3CR1^-EGFP^+$ cells in PGRP-S-dsRed/CX_3CR1-EGFP double transgenic mice (**Fig. 2B**). Correspondingly, in control mice lacking the PGRP-S-dsRed transgene, the red vesicles were absent, confirming that the red fluorescence was indeed from the dsRed reporter in M cells and not from autofluorescent material in the tissue (**Fig. 2C**). Furthermore, after the acquisition of the dsRed-labeled vesicles by dendritic cells, they remained segregated in a distinct cytoplasmic compartment (**Fig. 2D**). This phenomenon was also observed in the NALT (**Fig. 2E**), where basolateral vesicles were shed by M cells and were frequently seen within dendritic cell processes. To further characterize these structures, we stained Peyer's patches in order to detect the plasma membrane protein E-Cadherin, a transmembrane protein expressed by polarized epithelial cells (**Fig. 3**). We found that E-Cadherin is not present on these vesicles although they are clearly present in the M cell plasma membrane, suggesting that active sorting excludes this protein from the shed microvesicles. Based on the unique presence of these basolateral vesicles associated with mucosal M cells, we have termed these "M cell-derived microvesicles," or MCM.

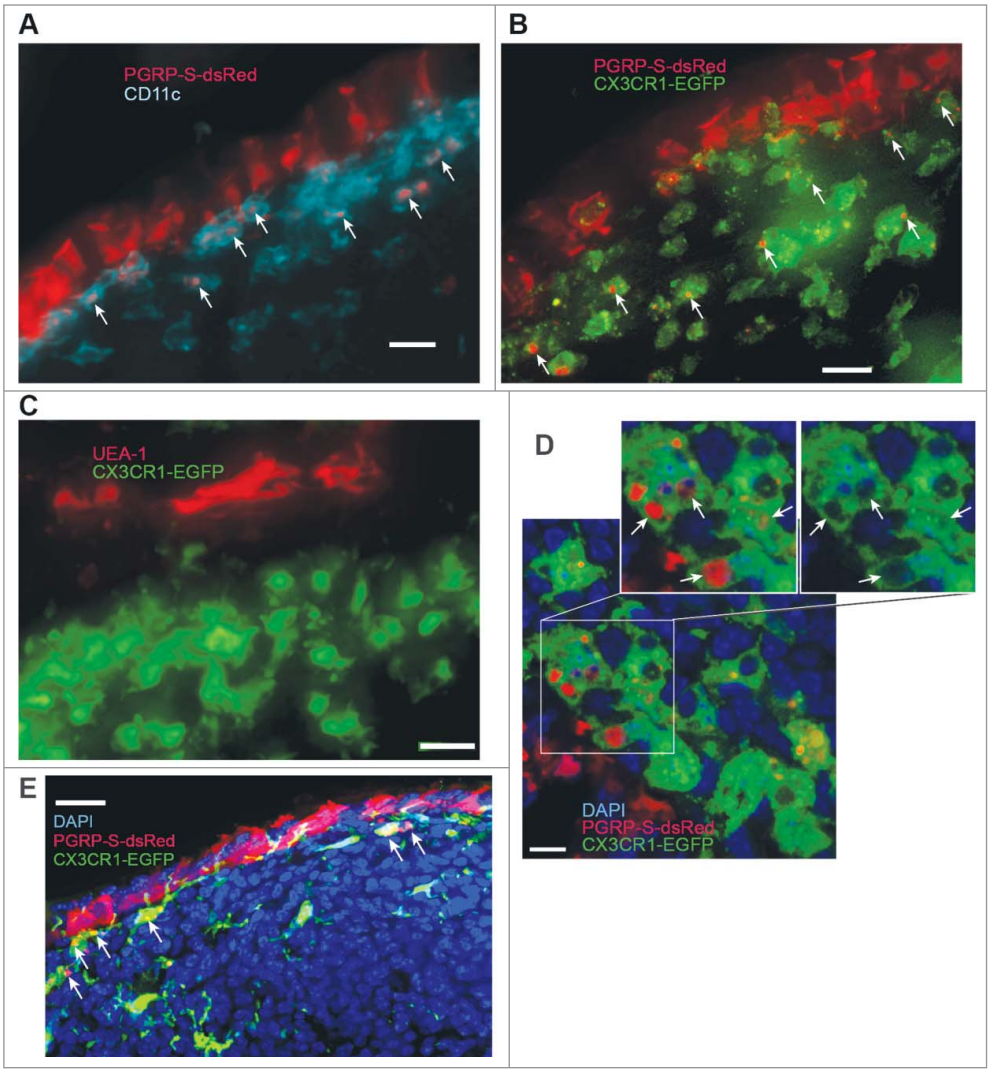

Figure 2. M cell expression of dsRed reveals vesicles in the subepithelial space. (**A**) PGRP-S-dsRed (red) identifies M cells (arrows). CD11c (blue) are dendritic cells. Scale bar: 40 μm. (**B**) PGRP-S-dsRed/CX_3CR1-EGFP mice show M cells/vesicles (arrows) (red) and myeloid cells (green). Scale bar: 10 μm. (**C**) CX_3CR1-EGFP mice, UEA-1 (red) stains apical membrane of M cells; green-myeloid cells. Scale bar: 20 μm. (**D**) Confocal of PGRP-S-dsRed/CX_3CR1-EGFP, vesicles (arrows); EGFP in dendritic cells; inset shows presence or absence of the red. DAPI (blue), M cell-derived vesicles [MCM] (red), and myeloid cells (green). Scale bar: 7 μm. (**E**) NALT M cells in PGRP-S-dsRed/CX_3CR1-EGFP mice: dsRed (red); vesicles (arrows); dendritic cells (green); nuclei DAPI (blue). Scale bar: 20 μm. Experiments were performed at least 3 times with an *n* of at least 3 for each group.

MCM are constitutively released independently of B cells and dendritic cells

Since B cells and dendritic cells play an important role in M cell development and function, we sought information on the role of these cell types on M cell vesicle shedding. In Igh-6^{tm1Cgn} mutant mice, which lack B lymphocytes due to a deletion in the Ig heavy chain gene, M cell lineage commitment is intact, but M cells fail to mature and acquire transcytosis function.[32] In mice with the PGRP-S-dsRed backcrossed onto the Igh-6 background, we were still able to detect the production of MCM and uptake by $CD11c^+$ dendritic cells (**Fig. 4**). Thus, vesicle release is independent from the formation of a basolateral pocket with B cells. Moreover, since M cell transcytosis is absent in these mice,

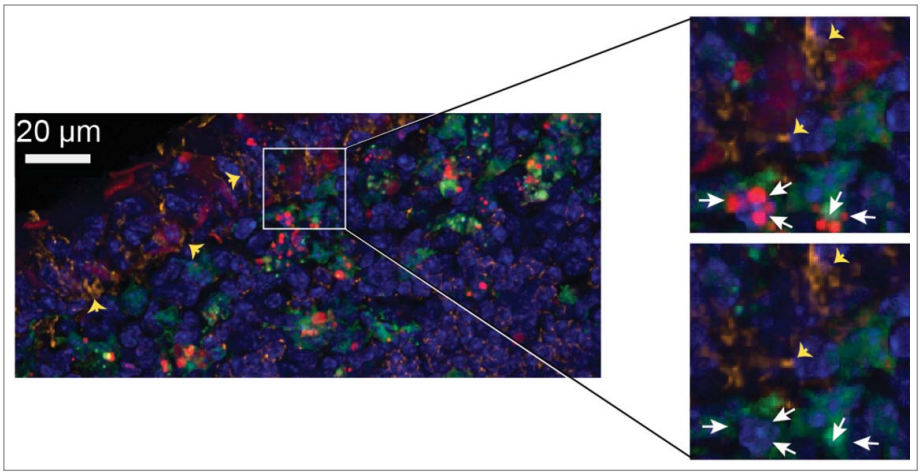

Figure 3. The plasma membrane protein E-Cadherin is not detectable on MCM. PGRP-S-dsRed/CX_3CR1-EGFP double transgenic mice were used. In the Peyer's patch (**A**), nuclei were stained with DAPI (blue) and anti-E-Cadherin (orange, yellow arrowheads) while M cells express dsRed (red, white arrows) and dendritic cells express EGFP (green). Scale bar: 20 μm. Experiments were performed at least 3 times with an *n* of at least 3 for each group.

MCM production was not dependent on functional maturation and uptake of luminal particles (**Fig.** 4).

The $dsRed^+$ cytoplasmic vesicles were nearly always found already within dendritic cells in the Peyer's patch subepithelial zone, suggesting that these vesicles were either very rapidly endocytosed by dendritic cells once shed by M cells, or alternatively, vesicle production might be specifically triggered by contact with the dendritic cells. To address this question, we injected mice with control liposomes (**Fig. 5A**, *top*) or clodronate liposomes (**Fig. 5A**, *bottom*) to deplete the subepithelial dendritic cells in the transgenic mice. Most Peyer's patches showed depletion of CX_3CR1-$EGFP^+$ (in double transgenic mice) and $CD11c^+$ cells (shown by immunofluorescence staining), although complete depletion of myeloid cells in Peyer's patch or intestinal villi was difficult to achieve. Regardless, clodronate depletion did generate large gaps between the M cells and underlying dendritic cells, and we found that free extracellular $dsRed^+$ vesicles were evident in the space below the M cells (**Fig. 5A**). These free vesicles were similar in size to the ones found within dendritic cells, suggesting that they are phagocytosed as intact cytoplasmic vesicles. In addition, many M cells could be seen with basolateral projections of cytoplasm extending into the subepithelial space, suggesting that vesicles may be budding off from these projections (**Fig. 5B**). Quantification of M cell cytoplasmic vesicles in liposome and clodronate injected mice supported the idea that the production of MCM was independent of CX_3CR1-$EGFP^+$ and $CD11c^+$ cells (**Fig. 5C**).

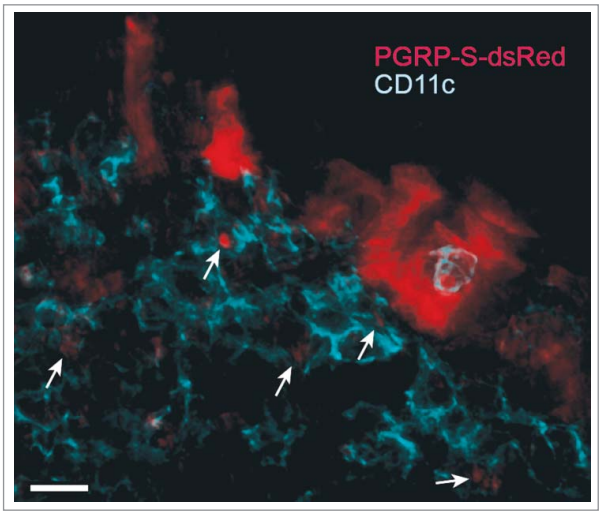

Figure 4. MCM are produced by immature M cells in Igh-6 mice. PGRP-S-$dsRed^+$/Igh-6 mutant mice (lacking B lymphocytes) were used to show MCM (arrows) were produced even in the absence of B cells; PGRP-S-dsRed (red) and CD11c (blue) identify M cells and dendritic cells, respectively. Scale bar: 20 μm. Experiments were performed at least 3 times with an *n* of at least 3 for each group.

To further identify the cells interacting with MCM, we performed immunofluorescence staining followed by confocal microscopy on PGRP-S-dsRed/CX_3CR1-EGFP double transgenic mice. Sections of Peyer's patches were stained using CD11b and CD11c antibodies (**Fig. 6A**). After quantification of CX_3CR1^+ cells in Volocity, we were able to identify approximately 81% as $CD11b^+$ and 11% as $CD11b^-$ (**Fig. 6B**) while 100% were $CD11c^+$ cells (**Fig. 6C**). These findings indicate that the population found to be CX_3CR1^+ are predominantly $CD11b^+CD11c^+$. Furthermore, these cells were also characterized based upon their association with $dsRed^+$ vesicles. Of the 81% $CX_3CR1^+CD11b^+$ cells, approximately 50% contain MCM while about 30% of the $CX_3CR1^+CD11b^-$ cells possessed MCM (**Fig. 6D**). Similarly to the $CX_3CR1^+CD11b^+$ cells, around 50% of all of the $CX_3CR1^+CD11c^+$ cells contain $dsRed^+$ vesicles (**Fig. 6E**). Taken together, these observations suggest that MCM are constitutively produced by the M cells themselves, independent of the presence of dendritic cells and B lymphocytes. Once shed, these vesicles are primarily taken up by $CX_3CR1^+CD11b^+CD11c^+$ cells.

MCM are preferentially found in dendritic cell compartments containing transcytosed bacteria

To examine the fate of the MCM, we performed uptake studies to compare their progression in the Peyer's patch with microbial particles or inert synthetic microparticles (**Fig.** 7). We performed intestinal loop uptake assays using polystyrene beads and 2 EGFP-expressing microbes (*Staphylococcus aureus* and *Yersinia entercolitica*), we found that bacteria were nearly always taken up by dendritic cells (**Fig. 7A**). Interestingly, the $dsRed^+$

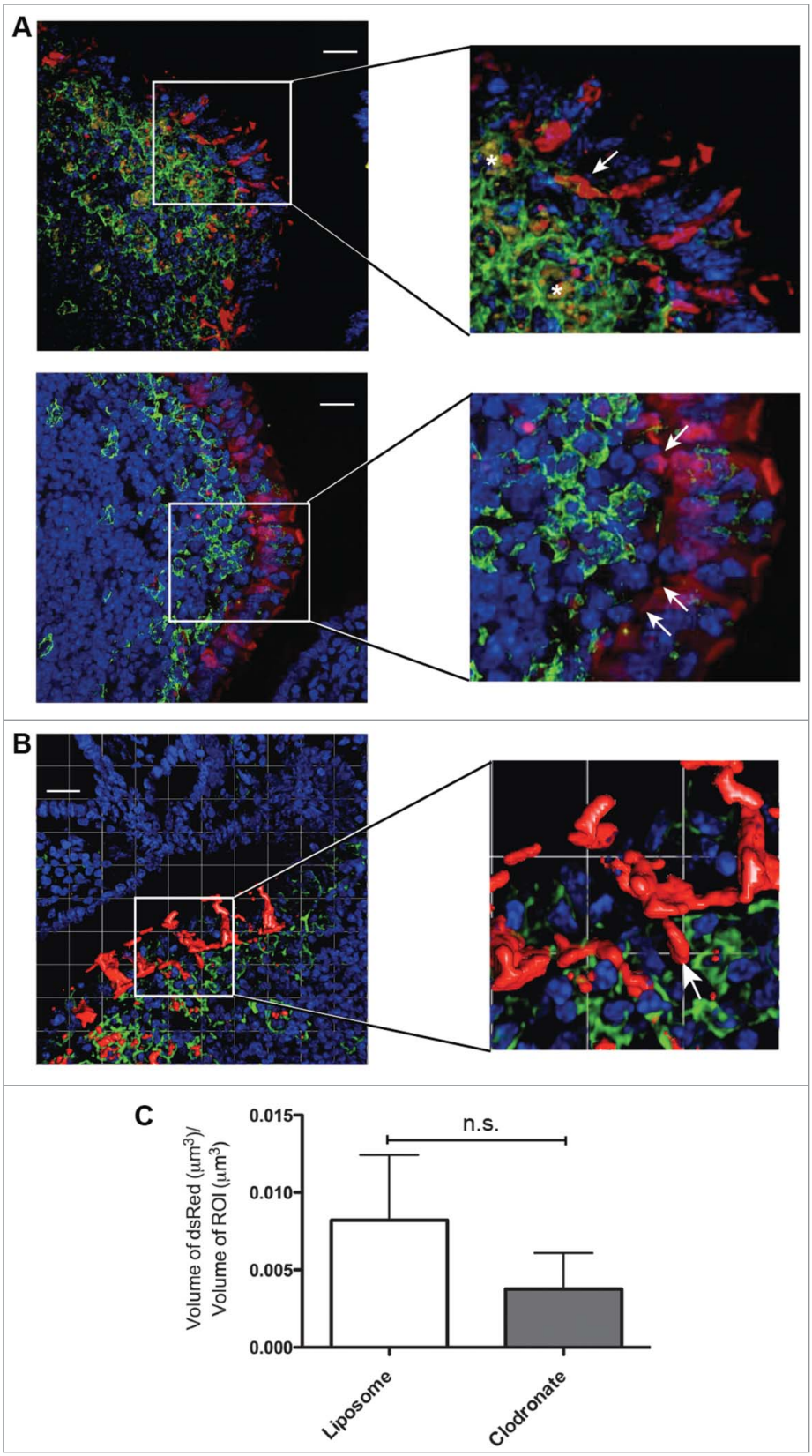

Figure 5. MCM are constitutively produced in clodronate treated transgenic mice. (**A, *top***) Non-clodronate (liposome) treated double transgenic mice and (**A, *bottom***) clodronate liposome treated (phagocyte depleted) mice were used to assess the role of phagocytic cells in vesicle production; dsRed cytoplasmic vesicles were evident (arrows) even after local depletion of myeloid cells. Scale bar: 21 μm. (**B**) 3D projection of confocal images clearly shows the production of MCM and basolateral protrusions (arrow) post-clodronate injection. Scale: 1 grid unit = 20 μm. (**C**) Quantification of dsRed vesicles in both liposome (*white bar*) and clodronate (*gray bar*) treated mice indicated that there was no statistically significant difference after dendritic cell reduction. Experiments were performed at least 3 times with an *n* of at least 3 for each group.

MCM were most commonly found inside the dendritic cell compartments along with the bacteria, unlike the polystyrene beads, which were mainly found in the subepithelial space outside of dendritic cells (**Figs. 7B and C**). The differing fates of these transcytosed particles indicated that while dsRed+ MCM were readily taken up by dendritic cells, they did not determine the fate of all transcytosed particles. Indeed, despite the preferential uptake of bacterial particles by dendritic cells, not all bacteria were associated with MCM. In a survey of images for uptake studies, we identified the proportions of dendritic cells in various categories: for a *S. aureus* uptake study, among 349 CD11+ dendritic cells examined in the Peyer's patch subepithelial zone, 80 (23%) contained both dsRed+ MCM and bacteria, 39 (11%) contained bacteria without MCM, and 30 (9%) contained MCM only. The remaining dendritic cells had neither bacterial particles nor MCM. For a *Salmonella* uptake study, among 209 CD11+ dendritic cells examined, 108 (52%) contained both dsRed+ MCM and bacteria, 42 (20%) contained bacteria without MCM, and 5 (2%) contained MCM alone. Thus, for 2 different uptake studies, MCM were not exclusively associated with M cell transfer of bacterial particle cargo to antigen presenting cells.

The uptake of the MCM by subepithelial dendritic cells and colocalization with transcytosed microbial particles suggests a unique role for MCM in the transfer of particles and antigens

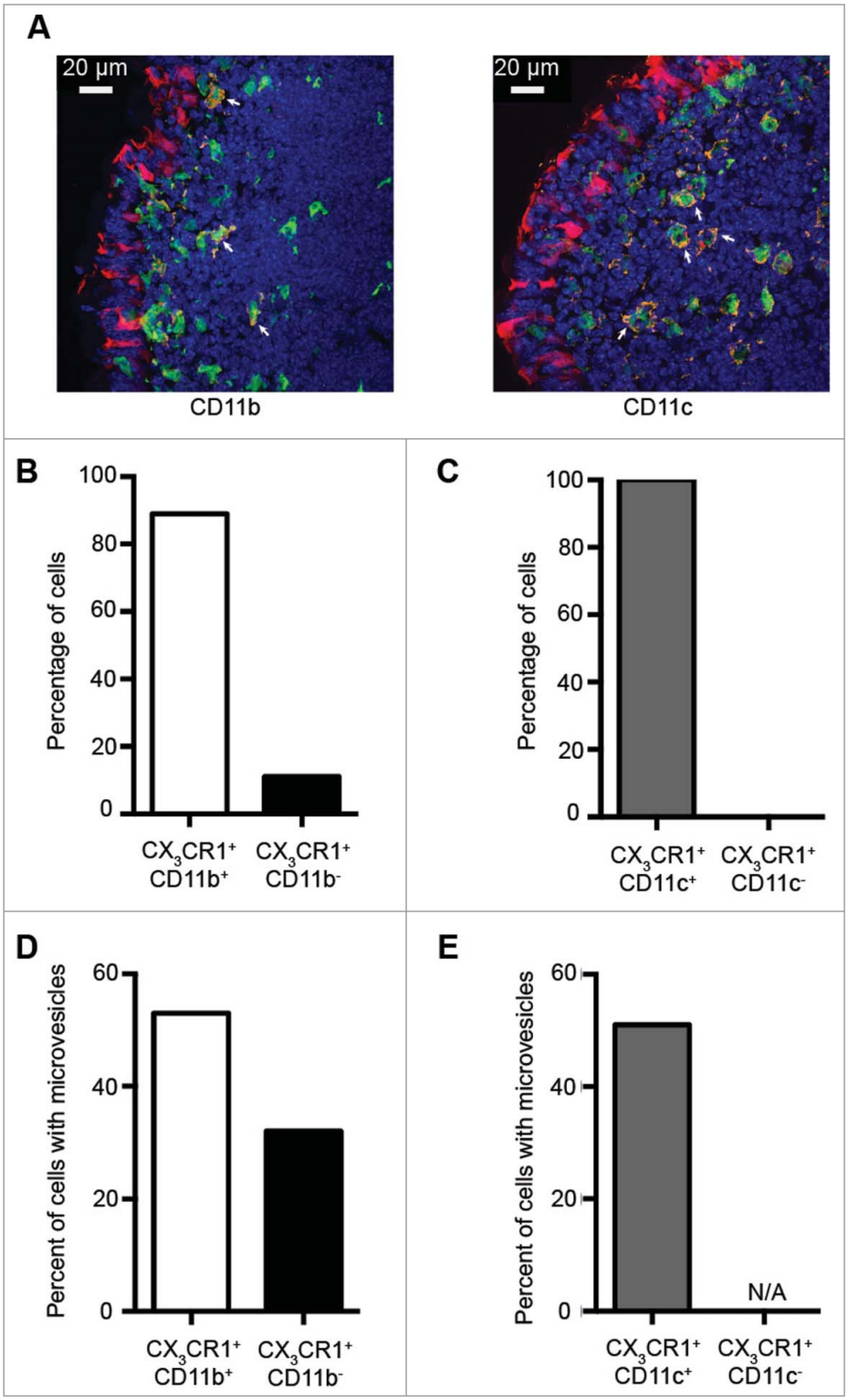

Figure 6. MCM primarily localize to $CX_3CR1^+CD11b^+CD11c^+$ cells in the subepithelial dome. Confocal microscopy images of Peyer's patches taken at 40x and stained with (**A, *left***) anti- CD11b (orange) and (**A, *right***) anti-CD11c (orange). Nuclei were stained with DAPI (blue), CX_3CR1^+ cells express EGFP (green), and M cells express dsRed (red). Using Volocity, percentages of (**B**) $CX_3CR1^+CD11b^+$ and $CX_3CR1^+CD11b^-$, as well as (**C**) $CX_3CR1^+CD11c^+$ and $CX_3CR1^+CD11c^-$ cells were determined. These subsets were further characterized based upon cells containing MCM. Percentages of cells associated with MCM for (**D**) $CX_3CR1^+CD11b^+$ and $CX_3CR1^+CD11b^-$ and (**E**) $CX_3CR1^+CD11c^+$ and $CX_3CR1^+CD11c^-$ are shown. Experiments were performed at least 3 times with an *n* of at least 8 for the analysis of each CD11b and CD11c.

from M cells to dendritic cells. To examine this issue, further detailed studies were done comparing the movement of microbial particles and MCM. In these studies, transcytosis across M cells was relatively rapid; fluorescent bacteria could be detected within M cells, as well as the underlying dendritic cells, as early as 10 minutes after infusion of the bacterial suspension into the intestinal lumen. We tested different types of $EGFP^+$ bacteria (*S. aureus, Salmonella enterica* serovar Typhimurium [*S. typhimurium*]), including both live and killed (either by heat or paraformaldehyde) at time points from 10 minutes to one hour. **Figure 8** shows the results with live *S. aureus* (**Fig. 8A**) and *S. typhimurium* (**Fig. 8B**), though similar results were obtained with killed microbes (not shown). Interestingly, transcytosis and dendritic cell uptake was frequently associated with dsRed vesicles. Bacteria transferred from M cells to subepithelial dendritic cells were, even at the earliest time points, associated with dsRed vesicles. In these images, when the green channel was removed, underlying dsRed was evident wherever EGFP signals were detected. The fluorescence patterns were not identical, suggesting slight differences in distribution of the bacteria versus M cell cytoplasmic dsRed, and also ruling out possible fluorescence channel cross-talk. By one hour after infusion of the bacteria, much of the green fluorescence was fairly diffuse, in many areas more evenly colocalizing with the dsRed signal in the dendritic cells (**Fig. 8C**). This may reflect fusion of the vesicles with lysosomes, and enzymatic degradation of the vesicle contents. Note that not all of the dsRed vesicles contained EGFP material, consistent with the notion that dsRed vesicle formation is constitutive, and not specifically dependent on the uptake of $EGFP^+$ bacteria. In sum, these studies show that the intake of MCM by dendritic

cells results in a similar (though not exclusive) fate as transcytosed luminal bacteria rather than with the polystyrene beads, suggesting a parallel function in inducing antigen specific mucosal immune responses.

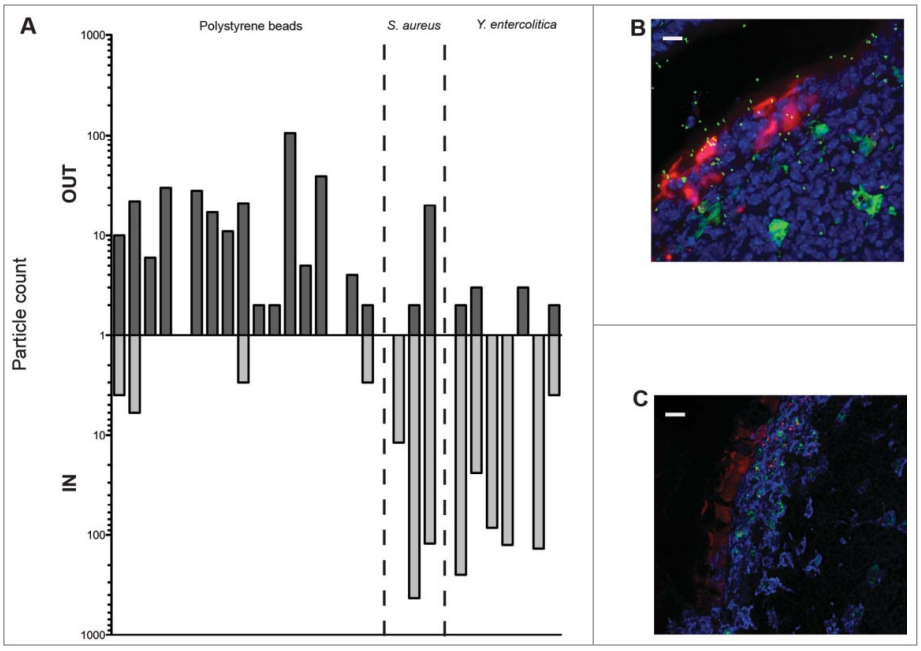

Figure 7. Transcytosed bacteria but not polystyrene beads preferentially localize in dendritic cell compartments. (**A**) Uptake in PGRP or PGRP-S-dsRed/CX_3CR1-EGFP mice using beads, *Staphylococcus aureus*, and *Yersinia entercolitica*. Each bar represents one image showing numbers of particles found in/out of dendritic cells. A nonparametric T-test was performed on ratios of particles found inside compared to outside of dendritic cells. *P*-value < 0.05 compared to beads for both *S. aureus* and *Y. entercolitica* (**B**) Image of beads. M cells (red); nuclei (blue); 1 μm AlexaFluor488 beads (green); EGFP-expressing myeloid cells (green). Scale bar: 10 μm. (**C**) Image of uptake using *S. aureus*; M cells (red); CD11c-stained dendritic cells (blue); EGFP- *S. aureus* (green). Scale bar: 16 μm. Experiments were performed at least 3 times with an *n* of at least 3 for each group.

Morphometric analysis of MCM production reveals regulation of vesicle characteristics by stimulation with bacteria

Although MCM production appeared to be independent of the presence of B cells and dendritic cells, it is possible that other factors can regulate the rate of production and size of the vesicles. Using image analysis, we found that there were indeed quantifiable differences in vesicle number and size depending on the type of microbes provided. We used image analysis to quantify differences in the vesicles. Vesicles were identified as distinct dsRed positive objects, using the automatic object identification feature of the image analysis software. The main finding from these studies (**Fig. 9**) was that the volumes of the large majority of the vesicles seen across all conditions were very similar on a whole population basis (**Fig. 9A**); as shown in the histogram, the vast majority of vesicles were measured to be smaller than approximately 6 μm^3. The median vesicle volume across all conditions (**Fig. 9B**) generally ranged from 2.8 μm^3 (*S. aureus*), to 3.4 μm^3 (unstimulated), to 3.9 μm^3 (*S. typhimurium*). This median vesicle volume appears to represent the bulk of the vesicles that are constitutively produced by the M cells.

Interestingly, in uptake studies using specific fluorescent microbe suspensions, the number of large MCM increased, raising the overall mean volume of the MCM. Here, the mean volume correlated with the estimated size of the microbes delivered in the vesicles (**Fig. 9C**). Thus, *S. aureus*-associated particles, estimated to be approximately 1 μm in diameter, generated the smallest MCM, with the mean volume similar to the constitutively produced vesicles in unstimulated mice ($\sim$15 μm^3). By contrast, *S. typhimurium*, estimated to be approximately 2 μm in length, generated the largest mean MCM volume ($\sim$40 μm^3). It is not clear whether the vesicles produced here reflect larger microbial particle diameters (with the flagellae of *S. typhimurium* adding to its effective particle volume), or whether this reflects the largest practical vesicles possible by this mechanism.

The cumulative effect of this increase in larger MCM volumes was also reflected in the calculated cumulative volume in vesicles as a percentage of each region of interest (ROI) in the subepithelial region. The unstimulated or PBS controls had the lowest ratio, with increasing cumulative vesicle volume as microbe size increased from lowest to highest (**Fig. 9D**): Unstimulated/PBS (0.019/0.016) < *S. aureus* (0.027) < *S. typhimurium* (0.040). This sequence may reflect both the differences in the average volume per vesicle induced by the various microbes, as well as relative stimulation of overall MCM production by microbial components.

Gram positive bacteria and a TLR2 agonist induce MCM shedding

While the addition of a suspension of microbes induced larger MCM, the total vesicle count per volume in the region below the follicle epithelium also increased with the addition of microbes, notably with the uptake of fluorescent *S. aureus* (**Fig. 10A**). This may be due to differences in the way the microbes interacted with the follicle epithelium, differences in virulence mechanisms, or other unknown factors. However, since not all MCM contained our injected microbial particles, we considered the possibility that other components within the microbes, such as innate immune ligands, might provide a more general stimulus for vesicle production. To support this, the concept that TLR2 stimulation enhances trancytosis of particles, such as polystyrene beads and vaccines, offered the possibility that TLR2 ligands may alter vesicle shedding.[33,34] To examine this question, we tested whether the TLR2 agonist Pam3CSK4 would be, by itself, sufficient to induce increased MCM formation, even in the absence

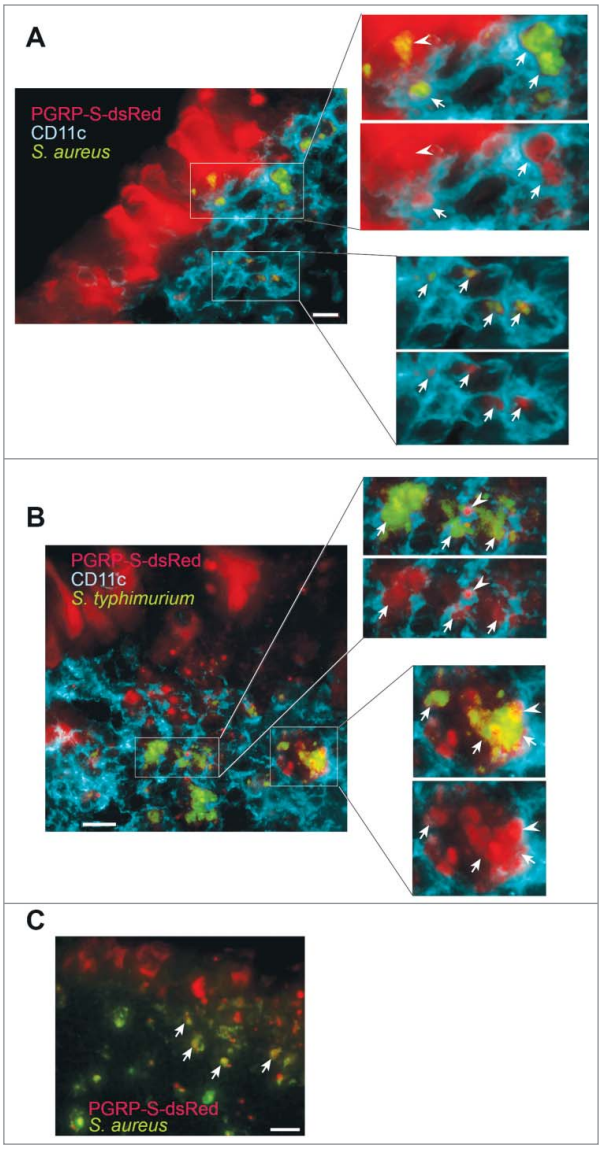

Figure 8. MCM preferentially localize in dendritic cell compartments containing transcytosed bacteria. PGRP-S-dsRed single transgenic mice were used to follow uptake of bacteria expressing EGFP (green). $CD11c^+$ dendritic cells are blue. Uptake after 15 minutes of *S. aureus* (**A**) and *S. typhimurium* (**B**); insets show colocalization of bacterial particles and $dsRed^+$ vesicles (arrows), seen with green channel on (upper image) or off (lower image). (**C**) Uptake after 60 minutes of *S. aureus*. Scale bars: **A** – 10 μm; **B** – 13 μm; **C** – 20 μm. Experiments were performed at least 3 times with an *n* of at least 3 for each group.

of added microbial particle suspensions (**Fig. 10B**). Interestingly, the addition of the TLR2 ligand significantly increased the production of basolateral MCM. Since no microparticles were injected into the intestinal lumen, there were no "cargo" particles available above those already potentially available in the intestinal lumen. Accordingly, the average size of the MCM remained small and were in fact found to be significantly smaller both by the median vesicle size (4.2 μm^3 for vehicle control vs. 2.9 μm^3 for Pam3CSK4) as well as the mean vesicle size (21 μm^3 for vehicle control versus 14 μm^3 for Pam3CSK4; $P < 0.0001$). To determine if this was specific for TLR2 we performed a ligated loop experiment with the TLR4 ligand LPS. Unlike stimulation with Pam3CSK4, LPS did not induce an increase in the number of vesicles released (**Fig. 10C**). Thus, while the production of MCM may be in part a general constitutive process, the nature and number of vesicles produced can be influenced by microbe-associated triggers such as the physical presence of microbial particles as well as TLR2 agonists.

Discussion

The uptake and transcytosis of microparticles by M cells has been known for decades, and many recent studies have used this phenomenon to examine the impact of various stimuli such as innate immune ligands on the rate of particle transcytosis by M cells *in vivo*.[35,36] In the present study, we found that the expression of a dsRed reporter protein in the cytoplasm of M cells gave us a new tool to follow the movement of mucosal luminal particles through M cells to underlying dendritic cells. Our findings suggest that M cells produce previously uncharacterized basolateral vesicles – MCM – that localize with bacteria within dendritic cells in the underlying follicle-associated epithelium.

The formation and shedding of these MCM could involve numerous proteins or pathways. Apoptotic machinery may be used in the formation and budding of these vesicles since apoptotic bodies are close in size to MCM.[37] Though their physical sizes are similar, there is one key aspect that distinguish apoptotic vesicles from MCM: organelle and nuclear fragments.[38] Our studies suggested that the vesicles did not label with reagents for detecting apoptotic blebs (not shown) and indeed, the associated M cell nuclei clearly remained intact without evidence for nuclear fragmentation. The observed vesicles are also possibly in the same category of vesicles as exosomes; they are both membrane bound vesicles released into extracellular space. Exosomes, as ESCRT-derived vesicular structures, are commonly associated with ubiquitinated and recycled proteins, while protein coats and SNARE proteins may play a role in promoting the freeing of these minute vesicles into the extracellular milieu.[39,40] The SNARE protein, syntaxin 4, has been observed to specifically target the basolateral plasma membrane of polarized cells, a region of particular interest for our MCM.[41] Unfortunately, mechanisms thought to be responsible for exosome production cannot account for the much larger MCM that are being generated. The apparent lack of E-Cadherin associated with the MCM suggests an active process that segregates cellular components as the MCM are produced, though at this point we do not have more specific information on what processes are involved. The mechanisms considered here do not provide clear candidates for the production of the MCM described here; while some components described above may be recruited for MCM production. It is also possible that other mechanisms not yet described are responsible. This study is the first to demonstrate this unique MCM, revealing more complex functions of this unique cell type. Additionally, our understanding of M cell capabilities as an antigen

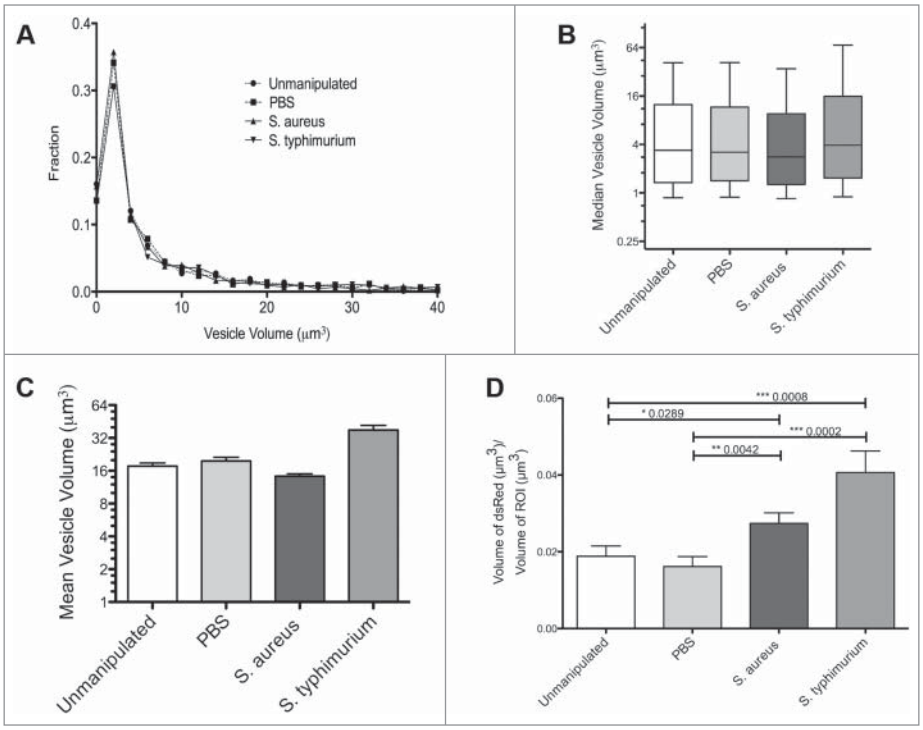

Figure 9. Quantification of vesicles during bacterial uptake shows that vesicle volume is mediated by cargo. (**A**) Histogram of the fraction of each vesicle volume. (**B**) Median of vesicle volume with interquartile range. (**C**) Mean vesicle volume (depicted as mean with SEM), showing slightly higher volume after uptake of *S. typhimurium*. (**D**) Volume of dsRed vesicles per region of interest (ROI) volume in the subepithelial region (shown as mean with SEM). Non-parametric *t*-test performed for each pairwise comparison. Experiments were performed at least 3 times with an *n* of at least 3 for each group.

delivering cell is extended by the identification of MCM playing a potential role in transcytosis.

Our findings demonstrating a preferential localization of MCM in dendritic cells with bacteria raises questions about the dynamics of microparticle delivery and the immune response associated with acquired antigen. MCM were rarely found in the subepithelial extracellular space such as the compartments containing transcytosed polystyrene beads, indicating that the fate of the MCM is clearly regulated with a preference for delivery to the same fate as transcytosed microorganisms, though this may be due to rapid uptake by dendritic cells through scavenger receptors rather than by any specific M cell-directed mechanism. In fact, the proportion of dendritic cells containing transcytosed bacteria, MCM, or both, could be consistent with independent uptake of particles vs. MCM rather than any coordinated specific uptake of MCM containing bacterial particles. Since MCM are composed of cytoplasmic contents, this raises the interesting possibility that MCM are perhaps more important for delivering soluble antigens entering the M cell cytoplasmic compartment, due to the release of microbial components or as a byproduct of intracellular infection.

Thus, the MCM could enable M cell packaging of cytosolic proteins necessary to coordinate a response to viruses, obligate intracellular bacteria, parasites, or even DNA vaccines.[42-44] This may be a mechanism for M cell subversion of evasion mechanisms utilized by viruses and intracellular microbes, such as *Listeria monocytogenes* and *Shigella flexneri*, and may also provide a mechanism to potentiate the effects of M cell-targeted vaccines.[43] Along the same lines, since M cells act as a funnel for luminal particles, possessing the ability to contain any dispersed microbial proteins is critical for the regulation of sampling and response elicitation. Furthermore, once these MCM are released, the efficiency of

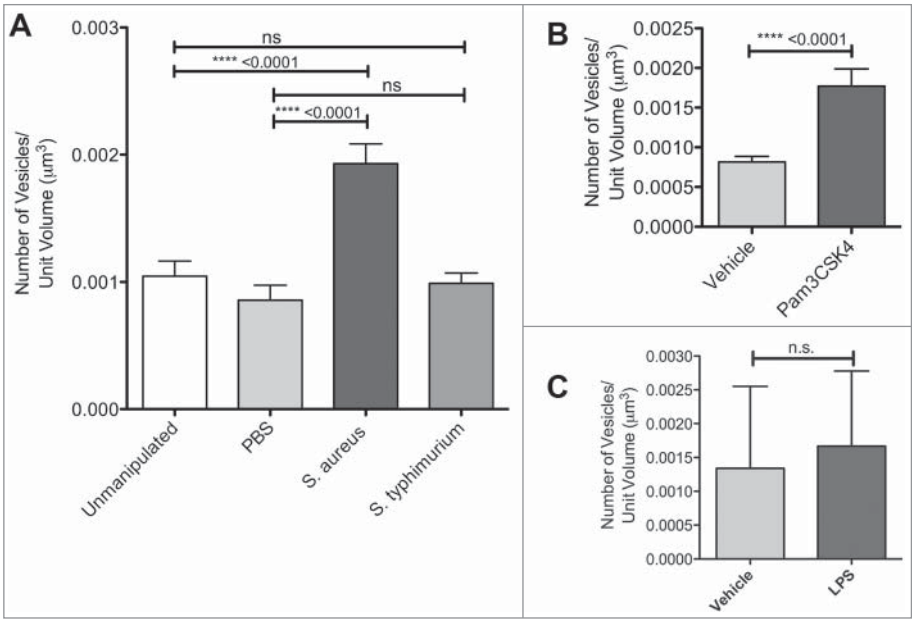

Figure 10. Gram positive bacteria and a TLR2 agonist influence the number of vesicles produced. (**A**) Number of vesicles counted per region of interest (ROI) in the subepithelial region (mean with SEM), showing increase when *S. aureus* was used. Non-parametric *t*-test performed for each pairwise comparison. Number of vesicles with (**B**) TLR2 and (**C**) TLR4 stimulation (mean with SEM) in the absence of labeled bacterial particles. Non-parametric *t*-test performed. Experiments were performed at least 3 times with an *n* of at least 3 for each group.

uptake by dendritic cells hints at the presence of scavenger receptor-mediated recognition and intake. Once released by M cells, MCM may rapidly display inner leaflet phosphatidylserine, mediating rapid capture by one of several scavenger receptors on dendritic cells; this has been a key mechanism promoting specific uptake of cargo such as apoptotic fragments by antigen presenting cells.[45]

Considering the role of M cells in the surveillance of luminal contents, understanding the context in which M cells promote immunogenic or tolerogenic responses is crucial. Since our study revealed constitutive shedding, as well as detection of vesicles in the same dendritic cell compartments as bacteria, we are inclined to postulate that MCM may play a dual role. M cells may constitutively release vesicles as a way to monitor and maintain natural gut microbiota and intestinal health, and mediate mucosal tolerance. In particular, the clear association of M cell vesicles with $CX_3CR1^+CD11b^+CD11c^+$ cells may hint at non-inflammatory behavior in the Peyer's patches, as it has been seen with this specific subpopulation of cells in the context of T-cell-dependent colitis.[46] Conversely, during an infection, an immunogenic response may be elicited for protection. Further characterization of these vesicles in normal and disease contexts may be key to establishing any potential role in immune surveillance and the maintenance of intestinal and mucosal homeostasis.

Materials and Methods

Mice

All mice were bred in the University of California, Riverside vivarium under specific pathogen-free conditions and were handled in accordance with Institutional Animal Care and Use Committee and National Institutes of Health guidelines. PGRP-S-dsRed or PGRP-S-dsRed/CX_3CR1-EGFP transgenic mice were used.[31] Male and female mice were between the ages of 2–3 months at the time of the experiment. Mice were fed ad libitum with an alfalfa-free diet in order to minimize any chlorophyll-related autofluorescence. In other studies we used Igh-6^{tm1Cgn} mutant mice backcrossed to BALB/c (recently renamed $Ighm^{tm1Cgn}$), which lack B lymphocytes due to a deletion in the Ig heavy chain gene.

Bacteria

5 ml of Luria-Bertani (LB) broth (Fisher BioReagents BP9723-500) was inoculated with *Staphylococcus aureus* strain RN4220 transformed with a green fluorescent protein (GFP) reporter plasmid (courtesy of A.R. Horswill), *Yersinia enterocolitica* (kindly provided by J. Mecsas), or *Salmonella enterica* serovar Typhimurium IR715 WT strain (courtesy of M. Raffatellu). The *Salmonella* strain was transformed with a vector containing EGFP (a gift from C.R. Nagler) using AMAXA nucleofector system. Bacteria were grown at 37°C and agitated at 250 RPM overnight. Uptake assays used 1×10^9 bacteria.

Clodronate liposome treatment

PGRP-S-dsRed/CX_3CR1- EGFP transgenic mice were administered either control liposomes or clodronate liposomes from Encapsome (SKU # 8901). Liposomes were brought to room temperature for 30 minutes prior to injections. Vials of liposomes were gently and thoroughly inverted in order to maintain a homogenous mixture. An intraperitoneal injection with 200 μl of 5 mg/ml of clodronate was performed every 2 days for a total of 3 injections within 6 days.

Uptake and TLR ligand experiments

PGRP-S-dsRed or PGRP-S-dsRed/CX_3CR1-EGFP transgenic mice were anesthetized with Avertin. A heat pad was used to maintain the body temperature of the mouse. The abdominal region was sterilized with 75% ethanol and surgical dress was placed over the animal. A 1 cm incision was made on the ventral-lateral side of the animal and a 5–7 cm portion of the small intestine was pulled out and tied off at either end with plastic string. For bacterial uptake, bacteria were washed 3 times with PBS. Bacteria was counted on a hemacytometer and resuspended in PBS for intraluminal injections. Approximately 500 μl (1×10^9 bacteria) of the bacterial suspension was injected along the length of the isolated intestine. PBS injections were used as a control for bacterial uptake experiments. Uptake was done for 15 minutes for *S. aureus* and *S. typhimurium*, 30 minutes for *Y. entercolitica*, or 1 hour for *S. aureus*. TLR2 stimulation with 200 μl of 1 mg/ml of Pam2CSK4 (InvivoGen), TLR4 stimulation with 200 μl of 100 μg/ml of LPS (Sigma), or endotoxin-free H_2O (control) was injected into the lumen of the intestine similarly to the bacterial injections for 10 minutes. TLR4 stimulation with LPS was done as previously described by Chabot et al.,[33] however, the time point was modified to stimulate uptake.

Sample preparation

Peyer's patches from the small intestine and nasal associated lymphoid (NALT) tissues were dissected from the mice. Tissues were fixed on ice in 4% paraformaldehyde with 30% sucrose in 1 × PBS for 1 hour. After, the tissue was placed in a mold with O. C.T compound (Tissue-tek 8345). The sample was flash frozen and sectioned by cryostat. 12–16 μm sections were made and tissues were placed on slides. Samples were stored at −20°C.

Immunofluorescence and confocal microscopy

Tissues were washed 3 × with 1 × PBS. Following the washes, sections were permeabilized with 0.5% Tween 20 (Fisher scientific BP337-100) in 1 × PBS for 10 minutes. After 2 washes with 0.1% Tween 20 in 1 × PBS (wash buffer), sections were blocked in 0.1% Tween in casein solution, and blocked with Avidin/biotin blocking kit (Vector SP-2001) if using a biotinylated antibody. Tissues were incubated in the following primary antibodies: 1:200 *Ulex europaeus* agglutinin 1 (UEA-1) lectin (Vector RL-1062), 1:100 CD11c (eBiosciences 13-0114-85), 1:100 CD45R/B220 (BD PharMingen 550286), and 1:100 E-Cadherin (Abcam 11512) for 2 hours at room temperature. Tissues were washed 3 × in wash buffer and incubated in secondary

antibody, 1:200 Streptavidin 647 (Life Technologies S32357), for 1 hour at room temperature. Slides were rinsed 3 × in wash buffer. Samples were post-fixed with 2% paraformaldehyde in 1 × PBS. Coverslips mounted with Prolong Gold antifade reagent with DAPI (Life technologies P36931). Slides were cured in the dark at room temperature for at least 24 hours. Images were obtained using a BD CARVII Confocal Imager (BD Biosystems) on a Zeiss Axio Observer inverted microscope. Original magnification of either 40x or 63x was used. Hardware control (microscope, confocal and digital camera; Diagnostic Instrument Xplorer–XS) and Metamorph Imaging Software. Image Z resolution was further optimized with Volocity software (PerkinElmer).

Confocal microscopy image quantification

Volocity was used for the quantification of CX_3CR1^+ cells that are characterized by CD11b, CD11c, and dsRed vesicles. Images used were of Peyer's patch sections. A region of interest (ROI) was designated as 100 μm below the basolateral edge of the M cells. Each cell type was identified based upon fluorescent color and average size using Volocity's Find Object (clipped to the ROI). Volocity's Find Object was further refined to separate CX_3CR1^+ cells that either contained CD11b or CD11c. Subsequently, this was repeated for vesicles.

For general vesicle identification, distinct dsRed positive objects were recognized using the automatic object identification feature of the Volocity image analysis software. Data was collected by individuals given images with coded file names blinded to the observers. The images were taken from just below the epithelial surface and extended 100 μm below the base of the M cells. Several parameters were assessed in ROI drawn in the area immediately below the follicle epithelium basement membrane: number of distinct vesicles per area, the average size of vesicles, and the volume of vesicles as a percentage of the ROI. For the same images Volocity's Find Object (clipped to the ROI) was used to find the average vesicle size as well as for finding the summed volume that the dsRed signal occupied. We limited the size threshold to objects above 0.7um and, for each picture intensity was adjusted to account for intensity of fluorescence between images and samples. The sum of the volume that the dsRed occupied was divided by the volume of the ROI to account for the difference in the number of stacks between images.

Comparison of particles found inside and outside of dendritic cells

Particle counts were performed using automated measurement parameters in Volocity (Find Objects and Compartmentalize protocols) where particles approximately 1 μm were counted and separated by their location (inside or outside of a dendritic cell). The region of interest extended up to approximately 100 μm below the follicle-associated epithelium.

Statistical analysis

All results where graphed and analyzed in GraphPad Prism 6 using a 2- tailed *t*-test. *P*-values less than 0.05 were considered significant.

Disclosure of Potential Conflicts of Interest

No potential conflicts of interest were disclosed.

Acknowledgments

We would like to thank A.R. Horswill for the green fluorescent protein (GFP) reporter, C.R. Nagler for the vector containing EGFP, J. Mecsas for *Yersinia enterocolitica*, and M. Raffatellu for *Salmonella enterica* serovar Typhimurium IR715 WT strain.

Funding

These studies were supported by NIH grants AI63426 and AI98973.

References

1. Hathaway LJ, Kraehenbuhl JP. The role of M cells in mucosal immunity. Cell Mol Life Sci 2000; 57:323-32; PMID:10766026; http://dx.doi.org/10.1007/PL00000693
2. Huang FP, Platt N, Wykes M, Major JR, Powell TJ, Jenkins CD, MacPherson GG. A discrete subpopulation of dendritic cells transports apoptotic intestinal epithelial cells to T cell areas of mesenteric lymph nodes. J Exp Med 2000; 191:435-44; PMID:10662789; http://dx.doi.org/10.1084/jem.191.3.435
3. Jung C, Hugot J-P, Barreau F. Peyer's patches: the immune sensors of the intestine. Int J Inflam 2010; 2010:823710; PMID:21188221; http://dx.doi.org/10.4061/2010/823710
4. Rescigno M, Urbano M, Valzasina B, Francolini M, Rotta G, Bonasio R, Granucci F, Kraehenbuhl JP, Ricciardi-Castagnoli P. Dendritic cells express tight junction proteins and penetrate gut epithelial monolayers to sample bacteria. Nat Immunol 2001; 2:361-7; PMID:11276208; http://dx.doi.org/10.1038/86373
5. McDole JR, Wheeler LW, McDonald KG, Wang B, Konjufca V, Knoop KA, Newberry RD, Miller MJ. Goblet cells deliver luminal antigen to CD103+ dendritic cells in the small intestine. Nature 2012; 483:345-9; PMID:22422267; http://dx.doi.org/10.1038/nature10863
6. Bennett KM, Walker SL, Lo DD. Epithelial microvilli establish an electrostatic barrier to microbial adhesion. Infect Immun 2014; 82:2860-2871; PMID:24778113; http://dx.doi.org/10.1128/IAI.01681-14
7. Neutra MR, Frey A, Kraehenbuhl JP. Epithelial M cells: gateways for mucosal infection and immunization. Cell 1996; 86:345-8; PMID:8756716; http://dx.doi.org/10.1016/S0092-8674(00)80106-3
8. Neutra MR, Mantis NJ, Frey A, Giannasca PJ. The composition and function of M cell apical membranes: implications for microbial pathogenesis. Semin Immunol 1999; 11:171-81; PMID:10381863; http://dx.doi.org/10.1006/smim.1999.0173
9. Asai T, Morrison SL. The SRC family tyrosine kinase HCK and the ETS family transcription factors SPIB and EHF regulate transcytosis across a human follicle-associated epithelium model. J Biol Chem 2013; 288:10395-405; PMID:23439650; http://dx.doi.org/10.1074/jbc.M112.437475
10. Hase K, Kawano K, Nochi T, Pontes GS, Fukuda S, Ebisawa M, Kadokura K, Tobe T, Fujimura Y, Kawano S, et al. Uptake through glycoprotein 2 of FimH(+) bacteria by M cells initiates mucosal immune response. Nature 2009; 462:226-30; PMID:19907495; http://dx.doi.org/10.1038/nature08529
11. Mabbott NA, Donaldson DS, Ohno H, Williams IR, Mahajan A. Microfold (M) cells: important immunosurveillance posts in the intestinal epithelium. Mucosal Immunol 2013; 6:666-77; PMID:23695511; http://dx.doi.org/10.1038/mi.2013.30
12. Nakato G, Hase K, Suzuki M, Kimura M, Ato M, Hanazato M, Tobiume M, Horiuchi M, Atarashi R, Nishida N, et al. Cutting edge: *Brucella abortus* exploits a cellular prion protein on intestinal M cells as an invasive receptor. J Immunol 2012; 189:1540-4; PMID:22772447; http://dx.doi.org/10.4049/jimmunol.1103332
13. Verbrugghe P, Waelput W, Dieriks B, Waeytens A, Vandesompele J, Cuvelier CA. Murine M cells express annexin V specifically. J Pathol 2006; 209:240-9; PMID:16552796; http://dx.doi.org/10.1002/path.1970
14. Rand JH, Wu X-X, Lin EY, Griffel A, Gialanella P, McKitrick JC. Annexin A5 binds to lipopolysaccharide and reduces its endotoxin activity. MBio 2012; 3:e00292-11; PMID:22415004; http://dx.doi.org/10.1128/mBio.00292-11
15. Rajapaksa TE, Stover-Hamer M, Fernandez X, Eckelhoefer HA, Lo DD. Claudin 4-targeted protein

incorporated into PLGA nanoparticles can mediate M cell targeted delivery. J Control Release 2010; 142:196-205; PMID:19896996; http://dx.doi.org/10.1016/j.jconrel.2009.10.033
16. Frey A, Neutra MR. Targeting of mucosal vaccines to Peyer's patch M cells. Behring Inst Mitt 1997; 98:376-89; PMID:9382762
17. Jones BD, Ghori N, Falkow S. *Salmonella typhimurium* initiates murine infection by penetrating and destroying the specialized epithelial M cells of the Peyer's patches. J Exp Med 1994; 180:15-23; PMID:8006579; http://dx.doi.org/10.1084/jem.180.1.15
18. Fujimura Y. Functional morphology of microfold cells (M cells) in Peyer's patches. Gastroenterol Jpn 1986; 21:325-34; PMID:3770353
19. Borghesi C, Regoli M, Bertelli E, Nicoletti C. Modifications of the follicle-associated epithelium by short-term exposure to a non-intestinal bacterium. J Pathol 1996; 180:326-32; PMID:8958813; http://dx.doi.org/10.1002/(SICI)1096-9896(199611)180:3%3c326::AID-PATH656%3e3.0.CO;2-6
20. Nicoletti C. Unsolved mysteries of intestinal M cells. Gut 2000; 47:735-9; PMID:11034595; http://dx.doi.org/10.1136/gut.47.5.735
21. Neutra MR, Pringault E, Kraehenbuhl JP. Antigen sampling across epithelial barriers and induction of mucosal immune responses. Annu Rev Immunol 1996; 14:275-300; PMID:8717516; http://dx.doi.org/10.1146/annurev.immunol.14.1.275
22. Hopkins SA, Niedergang F, Corthesy-Theulaz IE, Kraehenbuhl JP. A recombinant *Salmonella typhimurium* vaccine strain is taken up and survives within murine Peyer's patch dendritic cells. Cell Microbiol 2000; 2:59-68; PMID:11207563; http://dx.doi.org/10.1046/j.1462-5822.2000.00035.x
23. Macdonald TT, Monteleone G. Immunity, inflammation, and allergy in the gut. Science 2005; 307:1920-5; PMID:15790845; http://dx.doi.org/10.1126/science.1106442
24. Lo D. Cell culture modeling of specialized tissue: identification of genes expressed specifically by follicle-associated epithelium of Peyer's patch by expression profiling of Caco-2/Raji co-cultures. Int Immunol 2004; 16:91-9; PMID:14688064; http://dx.doi.org/10.1093/intimm/dxh011
25. Kernéis S, Bogdanova A, Kraehenbuhl JP, Pringault E. Conversion by Peyer's patch lymphocytes of human enterocytes into M cells that transport bacteria. Science 1997; 277:949-52; PMID:9252325; http://dx.doi.org/10.1126/science.277.5328.949
26. Gullberg E, Leonard M, Karlsson J, Hopkins AM, Brayden D, Baird AW, Artursson P. Expression of specific markers and particle transport in a new human intestinal M-cell model. Biochem Biophys Res Commun 2000; 279:808-13; PMID:11162433; http://dx.doi.org/10.1006/bbrc.2000.4038
27. Bhatnagar S, Shinagawa K, Castellino FJ, Schorey JS. Exosomes released from macrophages infected with intracellular pathogens stimulate a proinflammatory response *in vitro* and *in vivo*. Blood 2007; 110:3234-44; PMID:17666571; http://dx.doi.org/10.1182/blood-2007-03-079152
28. Lenassi M, Cagney G, Liao M, Vaupotic T, Bartholomeeusen K, Cheng Y, Krogan NJ, Plemenitas A, Peterlin BM. HIV Nef is secreted in exosomes and triggers apoptosis in bystander CD4+ T cells. Traffic 2010; 11:110-22; PMID:19912576; http://dx.doi.org/10.1111/j.1600-0854.2009.01006.x
29. Xiong J, Miller VM, Li Y, Jayachandran M. Microvesicles at the crossroads between infection and cardiovascular diseases. J Cardiovasc Pharmacol 2012; 59:124-32; PMID:21242813; http://dx.doi.org/10.1097/FJC.0b013e31820c6254
30. Timár CI, Lorincz AM, Csépányi-Kömi R, Vályi-Nagy A, Nagy G, Buzás EI, Iványi Z, Kittel A, Powell DW, McLeish KR, et al. Antibacterial effect of microvesicles released from human neutrophilic granulocytes. Blood 2013; 121:510-8; PMID:23144171; http://dx.doi.org/10.1182/blood-2012-05-431114
31. Wang J, Gusti V, Saraswati A, Lo DD. Convergent and divergent development among M cell lineages in mouse mucosal epithelium. J Immunol 2011; 187:5277-85; PMID:21984701; http://dx.doi.org/10.4049/jimmunol.1102077
32 Golovkina T V, Shlomchik M, Hannum L, Chervonsky A. Organogenic role of B lymphocytes in mucosal immunity. Science 1999; 286:1965-8; PMID:10583962; http://dx.doi.org/10.1126/science.286.5446.1965
33. Chabot S, Wagner JS, Farrant S, Neutra MR. TLRs regulate the gatekeeping functions of the intestinal follicle-associated epithelium. J Immunol 2006; 176:4275-83; PMID:16547265; http://dx.doi.org/10.4049/jimmunol.176.7.4275
34. Chabot SM, Chernin TS, Shawi M, Wagner J, Farrant S, Burt DS, Cyr S, Neutra MR. TLR2 activation by proteosomes promotes uptake of particulate vaccines at mucosal surfaces. Vaccine 2007; 25:5348-58; PMID:17582662; http://dx.doi.org/10.1016/j.vaccine.2007.05.029
35. Kim S-H, Seo K-W, Kim J, Lee K-Y, Jang Y-S. The M cell-targeting ligand promotes antigen delivery and induces antigen-specific immune responses in mucosal vaccination. J Immunol 2010; 185:5787-95; PMID:20952686; http://dx.doi.org/10.4049/jimmunol.0903184
36. Rajapaksa TE, Bennett KM, Hamer M, Lytle C, Rodgers VGJ, Lo DD. Intranasal M cell uptake of nanoparticles is independently influenced by targeting ligands and buffer ionic strength. J Biol Chem 2010; 285:23739-46; PMID:20511224; http://dx.doi.org/10.1074/jbc.M110.126359
37. Hristov M, Erl W, Linder S, Weber PC. Apoptotic bodies from endothelial cells enhance the number and initiate the differentiation of human endothelial progenitor cells *in vitro*. Blood 2004; 104:2761-6; PMID:15242875; http://dx.doi.org/10.1182/blood-2003-10-3614
38. Beyer C, Pisetsky DS. The role of microparticles in the pathogenesis of rheumatic diseases. Nat Rev Rheumatol 2010; 6:21-9; PMID:19949432; http://dx.doi.org/10.1038/nrrheum.2009.229
39. Saksena S, Sun J, Chu T, Emr SD. ESCRTing proteins in the endocytic pathway. Trends Biochem Sci 2007; 32:561-73; PMID:17988873; http://dx.doi.org/10.1016/j.tibs.2007.09.010
40. Cai H, Reinisch K, Ferro-Novick S. Coats, tethers, Rabs, and SNAREs work together to mediate the intracellular destination of a transport vesicle. Dev Cell 2007; 12:671-82; PMID:17488620; http://dx.doi.org/10.1016/j.devcel.2007.04.005
41. Breuza L, Fransen J, Le Bivic A. Transport and function of syntaxin 3 in human epithelial intestinal cells. Am J Physiol Cell Physiol 2000; 279:C1239-48; PMID:11003604
42. Wu Y, Wang X, Csencsits KL, Haddad A, Walters N, Pascual DW. M cell-targeted DNA vaccination. Proc Natl Acad Sci U S A 2001; 98:9318-23; PMID:11459939; http://dx.doi.org/10.1073/pnas.161204098
43. Jensen VB, Harty JT, Jones BD. Interactions of the invasive pathogens *Salmonella typhimurium*, *Listeria monocytogenes*, and *Shigella flexneri* with M cells and murine Peyer's patches. Infect Immun 1998; 66:3758-66; PMID:9673259
44. Deatherage BL, Cookson BT. Membrane vesicle release in bacteria, eukaryotes, and archaea: a conserved yet underappreciated aspect of microbial life. Infect Immun 2012; 80:1948-57; PMID:22409932; http://dx.doi.org/10.1128/IAI.06014-11
45. Kobayashi N, Karisola P, Peña-Cruz V, Dorfman DM, Jinushi M, Umetsu SE, Butte MJ, Nagumo H, Chernova I, Zhu B, et al. TIM-1 and TIM-4 glycoproteins bind phosphatidylserine and mediate uptake of apoptotic cells. Immunity 2007; 27:927-40; PMID:18082433; http://dx.doi.org/10.1016/j.immuni.2007.11.011
46. Kayama H, Ueda Y, Sawa Y, Jeon SG, Ma JS, Okumura R, Kubo A, Ishii M, Okazaki T, Murakami M, et al. Intestinal CX3C chemokine receptor 1(high) (CX3CR1(high)) myeloid cells prevent T-cell-dependent colitis. Proc Natl Acad Sci U S A 2012; 109:5010-5; PMID:22403066; http://dx.doi.org/10.1073/pnas.1114931109